Furthermore, the LPS- or hypothermia-induced cytokine production levels by the PBMCs showed marked elevation of IL-1β or IL-18 (Figs. 4a–c and 5b), as reported previously [16, 22]. The phenomena for hypothermic culture were similar to the findings in our recent report that NF-κB activity induced by LPS stimulation through TLR4 is enhanced in low-temperature cultures [23], although the precise mechanism of the association between the *NLRP3* variations and the low-temperature stimulation requires further clarification. These findings suggest that the cytokine production assays induced by LPS or hypothermia stimulation should be helpful for the diagnosis of FCAS. It should be noted that the serum IL-18 levels could be detected in all of the non-CAPS subjects, although the production levels of IL-18 from their PBMCs were lower than the detection limit. This might be dependent on the long half-life of IL-18 in human blood compared with the above-mentioned half-life of IL-1β.

The discrimination between CAPS and JIA cases is sometimes difficult because of their similar clinical characteristics. Interestingly, although case 5 had a rare missense variation in *NLRP3* (E378K) and some of her clinical symptoms were similar to those of CAPS (Table I), the E378K variant did not show enhancement of NK-κB activity (Fig. 2). This gene variation was inherited from her mother who did not show any inflammatory symptoms. Case 5 showed strong polyarthritis, continuous fever, and a recurrent generalized urticaria-like erythema as well as symptoms of CAPS. In particular, histopathological examination of a biopsy specimen from her skin rash revealed infiltration of neutrophils and mononuclear cells, representing similar findings to case 1 (Fig. 1). Thus, it was difficult to discriminate CAPS by the clinical symptoms alone in this case.

Therefore, to discriminate between CAPS and JIA in this case, we focused on her cytokine profiles. Her serum IL-6 and IL-18 levels were extremely high compared with not only the healthy controls but also the other CAPS patients (Fig. 3a, c). These observations resembled the serum cytokine pattern of systemic-onset JIA [21, 24]. Furthermore, the LPS-induced and hypothermia-induced IL-1β and IL-18 production levels by PBMCs from case 5 showed no increases compared with the control subjects (Figs. 4b, c and 5a, b). Recently, Saito et al. [5] reported that another screening method, LPS-induced monocyte cell death, was effective for diagnosing CAPS. The monocytes in case 5 did not show LPS-induced cell death. These objective results also supported the diagnosis of case 5 as JIA, rather than CAPS.

In this study, we evaluated several methods for the limited genotypes of patients with *NLRP3* variants. According to comparisons of the clinical phenotypes of previous case reports and our cases, the disease severity seems to be correlated with the serum cytokine levels and the ex vivo and in vitro responses and is almost completely determined by the specific mutations, which appear to suggest that other genetic or epigenetic determinants or environmental factors do not play a significant role.

Conclusions

A precise and easy method for the diagnosis of CAPS has not yet been established. The characteristics of the clinical phenotypes and the identification of proven gene variations of *NLRP3*, as the etiology of CAPS, are very important for diagnosing CAPS. In addition, the serum IL-18 levels and NF-κB activities of patients with the *NLRP3* variants reflect the phenotypes of disease severity. Evaluation of the cytokine profile is also a useful tool for diagnosing and discriminating the severity of CAPS.

Acknowledgements We thank the members of the families who agreed to participate in the study. We thank Dr. T. Fukao, Dr. M. Kawamoto, Dr. N. Kawamoto, and K. Kasahara for their advice and technical help. This work was supported by Grants-in-Aid for Scientific Research from the Ministry of Education, Science and Culture of Japan and by Health and Labour Science Research Grants for Research on Intractable Diseases from the Ministry of Health, Labour and Welfare.

Conflicts of Interest The authors have declared no conflicts of interest.

References

1. Hoffman HM, Simon A. Recurrent febrile syndromes: what a rheumatologist needs to know. Nat Rev Rheumatol. 2009;5:249–56.
2. Aksentijevich I, Nowak M, Mallah M, Chae JJ, Watford WT, Hofmann SR, et al. De novo CIAS1 mutations, cytokine activation, and evidence for genetic heterogeneity in patients with neonatal-onset multisystem inflammatory disease (NOMID): a new member of the expanding family of pyrin-associated autoinflammatory diseases. Arthritis Rheum. 2002;46:3340–8.
3. Feldmann J, Prieur AM, Quartier P, Berquin P, Certain S, Cortis E, et al. Chronic infantile neurological cutaneous and articular syndrome is caused by mutations in CIAS1, a gene highly expressed in polymorphonuclear cells and chondrocytes. Am J Hum Genet. 2002;71:198–203.
4. Hoffman HM, Mueller JL, Broide DH, Wanderer AA, Kolodner RD. Mutation of a new gene encoding a putative pyrin-like protein causes familial cold autoinflammatory syndrome and Muckle–Wells syndrome. Nat Genet. 2001;29:301–5.
5. Saito M, Nishikomori R, Kambe N, Fujisawa A, Tanizaki H, Takeichi K, et al. Disease-associated CIAS1 mutations induce monocyte death, revealing low-level mosaicism in mutation-negative cryopyrin-associated periodic syndrome patients. Blood. 2008;111:2132–41.
6. Tanaka N, Izawa K, Saito MK, Sakuma M, Oshima K, Ohara O, et al. High incidence of NLRP3 somatic mosaicism in chronic infantile neurological cutaneous and articular syndrome patients: the

results of an international multicenter collaborative study. Arthritis Rheum. 2011;63:3625–32.
7. Saito M, Fujisawa A, Nishikomori R, Kambe N, Nakata-Hizume M, Yoshimoto M, et al. Somatic mosaicism of CIAS1 in a patient with chronic infantile neurologic, cutaneous, articular syndrome. Arthritis Rheum. 2005;52:3579–85.
8. Matsubayashi T, Sugiura H, Arai T, Oh-Ishi T, Inamo Y. Anakinra therapy for CINCA syndrome with a novel mutation in exon 4 of the CIAS1 gene. Acta Paediatr. 2006;95:246–9.
9. Jeru I, Duquesnoy P, Fernandes-Alnemri T, Cochet E, Yu JW, Lackmy-Port-Lis M, et al. Mutations in NALP12 cause hereditary periodic fever syndromes. Proc Natl Acad Sci USA. 2008;105:1614–9.
10. Jeru I, Marlin S, Le Borgne G, Cochet E, Normand S, Duquesnoy P, et al. Functional consequences of a germline mutation in the leucine-rich repeat domain of NLRP3 identified in an atypical autoinflammatory disorder. Arthritis Rheum. 2010;62:1176–85.
11. Church LD, Savic S, McDermott MF. Long term management of patients with cryopyrin-associated periodic syndromes (CAPS): focus on rilonacept (IL-1 Trap). Biologics. 2008;2:733–42.
12. Yamauchi A, Iwata H, Ohnishi H, Teramoto T, Kondo N, Seishima M. Interleukin-17 expression in the urticarial rash of familial cold autoinflammatory syndrome: a case report. Br J Dermatol. 2010;163:1351–3.
13. Petty RE, Southwood TR, Baum J, Bhettay E, Glass DN, Manners P, et al. Revision of the proposed classification criteria for juvenile idiopathic arthritis: Durban, 1997. J Rheumatol. 1998;25:1991–4.
14. Milhavet F, Cuisset L, Hoffman HM, Slim R, El-Shanti H, Aksentijevich I, et al. The infevers autoinflammatory mutation online registry: update with new genes and functions. Hum Mutat. 2008;29:803–8.
15. Caroli F, Pontillo A, D'Osualdo A, Travan L, Ceccherini I, Crovella S, et al. Clinical and genetic characterization of Italian patients affected by CINCA syndrome. Rheumatol Oxford. 2007;46:473–8.
16. Rosengren S, Mueller JL, Anderson JP, Niehaus BL, Misaghi A, Anderson S, et al. Monocytes from familial cold autoinflammatory syndrome patients are activated by mild hypothermia. J Allergy Clin Immunol. 2007;119:991–6.
17. Hoffman HM, Wanderer AA, Broide DH. Familial cold autoinflammatory syndrome: phenotype and genotype of an autosomal dominant periodic fever. J allergy clin immunol. 2001;108:615–20.
18. Kambe N, Satoh T, Tanizaki H, Fujisawa A, Saito MK, Nishikomori R. Enhanced NF-kappaB activation with an inflammasome activator correlates with disease activity of NLRP3 mutations outside of exon 3: comment on an article by Jeru et al. Arthritis Rheum. 2010;62:3123–4.
19. Madhok R, Crilly A, Watson J, Capell HA. Serum interleukin 6 levels in rheumatoid arthritis: correlations with clinical and laboratory indices of disease activity. Ann Rheum Dis. 1993;52:232–4.
20. Tanaka H, Miyazaki N, Oashi K, Teramoto S, Shiratori M, Hashimoto M, et al. IL-18 might reflect disease activity in mild and moderate asthma exacerbation. J Allergy Clin Immunol. 2001;107:331–6.
21. Lotito AP, Campa A, Silva CA, Kiss MH, Mello SB. Interleukin 18 as a marker of disease activity and severity in patients with juvenile idiopathic arthritis. J Rheumatol. 2007;34:823–30.
22. Janssen R, Verhard E, Lankester A, Ten Cate R, van Dissel JT. Enhanced interleukin-1beta and interleukin-18 release in a patient with chronic infantile neurologic, cutaneous, articular syndrome. Arthritis Rheum. 2004;50:3329–33.
23. Arai T, Kaneko H, Ohnishi H, Matsui E, Fukao T, Kawamoto N, et al. Hypothermia augments NF-kappaB activity and the production of IL-12 and IFN-gamma. Allergol Int. 2008;57:331–8.
24. Yilmaz M, Kendirli SG, Altintas D, Bingol G, Antmen B. Cytokine levels in serum of patients with juvenile rheumatoid arthritis. Clin Rheumatol. 2001;20:30–5.

CLINICAL REPORT

Cryopyrin-associated Periodic Syndrome: A Case Report and Review of the Japanese Literature

Kumi AOYAMA[1], Hiroo AMANO[1], Yuki TAKAOKA[2], Ryuta NISHIKOMORI[2] and Osamu ISHIKAWA[1]
[1]Department of Dermatology, Gunma University Graduate School of Medicine, Maebashi, Gunma and [2]Department of Pediatrics, Kyoto University Graduate School of Medicine, Kyoto, Japan

Cryopyrin-associated periodic syndrome is an autoinflammatory syndrome caused by mutations of the *CIAS1* gene (currently named *NLRP3*), and is characterized by periodic attacks of an urticaria-like rash, fever, headache, conjunctivitis and arthralgia. We report here a case of a 1-year-old boy with cryopyrin-associated periodic syndrome, which manifested as a recurrent skin rash in the postnatal period. Genetic analysis revealed a missense mutation of the *CIAS1* gene in the mother and infant. ***Key words: cryopyrin-associated periodic syndrome; urticaria-like rash, NLRP3.***

(Accepted November 14, 2011.)

Acta Derm Venereol 2012; 92: XX–XX

Kumi Aoyama, Department of Dermatology, Gunma University Graduate School of Medicine, 3-39-22 Showa-machi, Maebashi, Gunma 371-8511, Japan. E-mail: kumako@ac.auone-net.jp

Cryopyrin-associated periodic syndrome (CAPS) is an autoinflammatory syndrome caused by mutations in *NLRP3* encoding cryopyrin (1). Three clinical types exist: familial cold autoinflammatory syndrome (FCAS), Muckle-Wells syndrome (MWS) and chronic infantile neurological, cutaneous and articular (CINCA) syndrome (1–4). FCAS is an autosomal dominant inflammatory disease and the least severe phenotype characterized by recurrent episodes of skin rash, fever, arthralgia and conjunctivitis after generalized exposure to cold (2). MWS is characterized by progressive sensorineural deafness as well as recurrent episodes of skin rash, fever and arthralgia (1). CINCA has the most severe phenotype with clinical features mimicking those of juvenile rheumatoid arthritis, including early onset, recurrent episodes of skin rash, fever, arthralgia, central nervous system involvement, and occasionally, a fatal outcome in the first or second decade of life (4).

We report here a case of CAPS in a Japanese male infant and review the clinical characteristics of the 19 cases of CAPS reported in Japanese patients.

CASE REPORT

A 1-year-old boy with a skin rash was referred to our hospital in April 2010. The skin rash appeared immediately after birth, recurred intermittently, and was not relieved by antihistamines. It was unclear whether the infant had itching. The patient's mother and maternal grandmother also had a history of a similar urticaria-like rash without itching, associated with periodic high fever of unknown origin and arthralgia. On physical examination, urticaria-like plaques 10–20 mm in diameter surrounded by erythema were distributed across the cheeks and upper and lower extremities (Fig. 1). Audiography was normal and no swollen joints were seen. Haematological examination revealed a red blood cell count of $5.53 \times 10^6/\mu l$ and a platelet count of $415 \times 10^3/\mu l$, with the white blood cell count (7,900/μl) and C-reactive protein (0.02 mg/dl) within normal limits. Levels of serum amyloid A (SAA), interleukin (IL)-1β and IL-6 were not elevated and autoantibodies including antinuclear antibodies, anti-SS-A, anti-SS-B and rheumatoid factor were negative. Although the parents did not consent to a skin biopsy for histopathological examination, they did consent to investigation of *NLRP3* mutation analysis using blood samples taken from the patient and his mother. A heterozygous nucleotide transition C1316T (cytosine-to-thymine transition at position 1316) was detected in exon 3 of *NLRP3*,

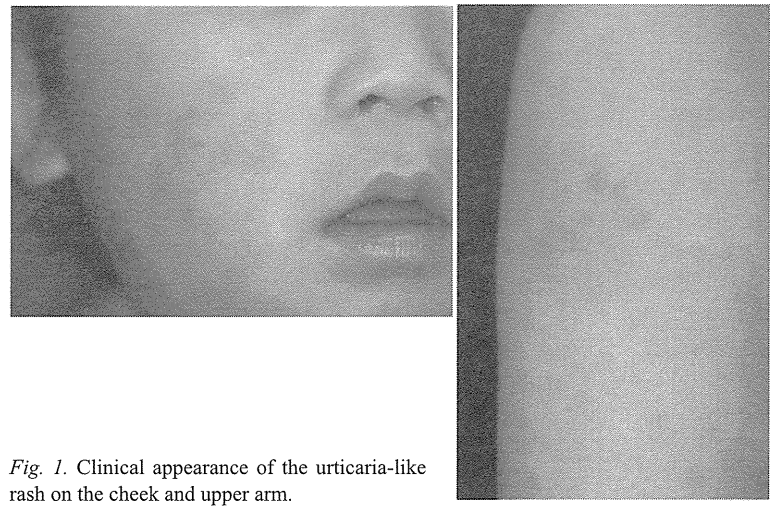

Fig. 1. Clinical appearance of the urticaria-like rash on the cheek and upper arm.

 doi: 10.2340/00015555-1322
 ISSN 0001-5555

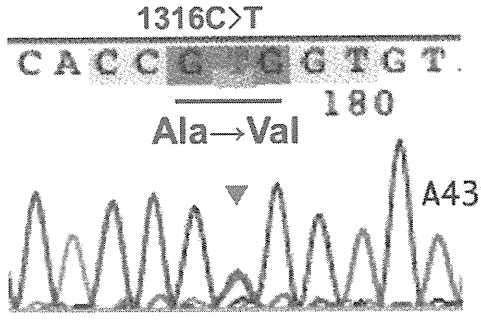

Fig. 2. Chromatograms of the *NLRP3* gene at position 1316, obtained from *NLRP3* gene analysis of the patient. The arrowhead indicates position 1316 on the patient's chromatogram.

resulting in a novel A439V (substitution of alanine by valine at position 439) amino acid replacement in the NOD domain (Fig. 2). The mother also had the same mutation. In light of the gene mutation analysis findings, together with the clinical features, we made the diagnosis of FCAS.

DISCUSSION

Systemic autoinflammatory diseases, a recently established disease concept, are characterized by recurrent episodes of inflammation in the absence of infectious and autoimmune causes. This category includes the hereditary periodic fever syndromes, namely, familial Mediterranean fever (FMF), tumour necrosis factor receptor-associated periodic fever syndrome (TRAPS), hyperimmunoglobulinaemia D with periodic fever syndrome and cryopyrinopathies (CAPS). Moreover, other classifications have been proposed that include diseases such as Blau syndrome, Behçet's disease and Crohn's disease (5–8).

CAPS is caused by a mutation in the *CIAS1/NLRP3* gene. *NLRP3* plays a critical role in innate immunity, as it responds to intracellular pathogens and some hazardous signals. NLRP3 participates in the formation of the inflammasome, a multiprotein complex including an NLR (a Nod-like receptor) protein and an adaptor protein called apoptosis-associated speck-like protein containing a caspase recruitment and activating domain (ASC). The ASC binds and activates procaspase-1 (9, 10). Activation of the inflammasome results in conversion of pro-caspase-1 into the active protease, caspase-1, leading to caspase-1-mediated cleavage of its target molecules, such as pro-IL-1β and pro-IL-18, into biologically active forms. These cytokines participate in systemic and local responses to infection or injury (9–14). Although these cytokines can induce an urticaria-like rash, patients usually do not experience itching as there is no histamine release (15).

We reviewed 19 cases of Japanese patients with a diagnosis of CAPS (16–29). The clinical symptoms and laboratory findings are summarized in Table I.

Table I. Clinical symptoms and laboratory findings in 19 Japanese patients with cryopyrin-associated periodic syndrome

Author, year (Ref.)	Disease	Age/sex	Age at onset	Symptom of onset	Family history	Gene analysis	Fever	Joint involvement	Eye involvement	Amyloidosis	Deafness	Chronic meningitis
Tamaki et al. 1976 (16)	MWS	35 years/M	3 years	Urticarial rash	+	ND	+	+	+	ND	+	–
	MWS	1 year/F	3 months	Urticarial rash	+	ND	ND	ND	+	ND	–	ND
	FCAS	31 years/F	2 years	Skin rash	+	ND	+	+	+	ND	ND	ND
Yamashita et al. 1987 (17)	FCAS	3 years/M	2 months	Skin rash	+	ND	+	–	+	ND	ND	ND
	CINCA	14 years/M	At birth	Skin rash	ND	ND	+	+	ND	ND	ND	+
Inamo et al. 1994 (18)	CINCA	15 years/M	At birth	Fever, lymph node enlargement	ND	ND	+	+	+	ND	+	ND
Miura et al. 1997 (19)	CINCA	0 months/F	At birth	Abdominal distension, bilious vomiting	–	ND	+	+	+	ND	ND	ND
Mori et al. 2002 (20)	CINCA	7 years/M	2 weeks	Fever	ND	ND	+	+	ND	ND	+	+
Saito et al. 2005 (21)	CINCA	15 years/M	1 year	Arthritis of the knee	–	S196N, Y570C	ND	+	+	ND	+	+
Gotoh et al. 2006 (22)	CINCA	1 year/F	At birth	CRP(+), skin rash	–	+	+	–	+	ND	–	+
Matsubara et al. 2006 (23)	CINCA	10 months/M	At birth	Fever, skin rash	ND	G307V	+	+	ND	+	+	–
Koike et al. 2007 (24)	MWS	23 years/F	Childhood	Fever, conjunctivitis, urticarial rash	–	H312P	+	+	+	+	+	ND
Fujisawa et al. 2007 (25)	MWS	12 years/M	3rd days	Urticarial rash	+	R260W	ND	–	ND	+	ND	+
Kawashima et al. 2007 (26)	CINCA	11 years/M	At birth	Fever	ND	–	+	+	–	ND	+	+
Itazawa et al. 2008 (27)	FCAS	14 years/F	4 month	Urticarial rash	+	R260W	+	+	+	+	ND	ND
Miyamae et al. 2010 (28)	CINCA	10 months/F	10 month	Fever, growth disorder	–	–	+	+	ND	ND	ND	–
Yamauchi et al. 2010 (29)	FCAS	34 years/M	Infancy	Skin rash	+	Y563N	ND	ND	+	–	–	–
Our case	FCAS	1 month/M	At birth	Urticaria-like rash	+	A439V	–	–	–	–	–	–
His mother	FCAS	34 years/F	At birth	Urticaria-like rash	+	A439V	+	+	+	–	–	–

MWS: Muckle-Wells syndrome; CINCA: chronic infantile neurological, cutaneous, articular syndrome; FCAS: familial cold autoinflammatory syndrome; CRP: C-reactive protein; ND: not described.

Eleven patients were male and 8 patients were female, in which 6 patients had FCAS, 4 had MWS and 9 had CINCA. Symptoms of CAPS first appeared during early childhood (0–3 years old), with skin rash being the most frequent initial symptom ($n=12$). Regardless of the nature of the initial symptom, all patients developed the characteristic, recurrent urticaria-like rash, with the second most common symptom being periodic high fever ($n=14$), followed by arthralgia and arthritis ($n=13$). Other clinical features included ocular involvement (optic nerve atrophy, chorioretinitis, uveitis (conjunctivitis)) in 12 patients, elevated levels of serum SAA in 4 patients, and deafness in 7 patients. A family history of recurrent autoinflammatory syndrome was identified in 6 cases, although it was noted that a family history was not described in 4 cases. With regard to genetic analysis, *NLRP3* mutations were detected in 9 of 10 patients investigated, with one patient exhibiting *NLRP3* somatic mosaicism. Somatic mosaicism of *NLRP3* may result in a relatively mild phenotype of CINCA compared with common *NLRP3* mutations, attributable to the difference in genotype expression among different somatic cells, namely, fewer cells in the central nervous system express the active mutation compared with those in skin (21).

An urticaria-like rash is a typical feature of CAPS, which may be encountered by dermatologists and paediatricians, and has a high risk of frequent misdiagnosis. When infants or toddlers present with an urticaria-like rash, practitioners should recall CAPS as a differential diagnosis and examine the recurrent bouts of unprovoked inflammation in various organs other than the skin.

ACKNOWLEDGEMENT

We thank Dr Naotomo Kambe (Chiba University) for helpful suggestions.

The authors declare no conflicts of interest.

REFERENCES

1. Hoffman HM, Mueller JL, Broide DH, Wanderer AA, Kolodner RD. Mutation of a new gene encoding a putative pyrin-like protein causes familial cold autoinflammatory syndrome and Muckle-Wells syndrome. Nat Genet 2001; 29: 301–305.
2. Hoffman HM, Wanderer AA, Broide DH. Familial cold autoinflammatory syndrome: Phenotype and genetype of an autosomal dominant periodic fever. J Allergy Clin Immunol 2001; 108: 615–620.
3. Manji GA, Wang L, Geddes BJ, Brown M, Merriam S, Al-Garawi A, et al. PYPAF1, A PYRIN-containing Apaf1-like protein that assembles with ASC and regulates activation of NF-κB. J Biol Chem 2002: 277: 11570–11575.
4. Feldmann J, Prieur AM, Quartier P, Berquin P, Certain S, Cortis E, et al. Chronic infantile neurological cutaneous and articular syndrome is caused by mutations in CIAS1, a gene highly expressed in polymorphonuclear cells and chondrocytes. Am J Hum Genet 2002; 71: 198–203.
5. Kastner DL, Aksentijevich I, Goldbach-Mansky R. Autoinflammatory disease reloaded: a clinical perspective. Cell 2010; 140: 784–790.
6. Farasat S, Aksentijevich I, Toro JR. Autoinflammatory diseases: clinical and genetic advances. Arch Dermatol 2008; 144: 392–402.
7. Galon J, Aksentijevich I, McDermott MF, O'Shea JJ, Kastner DL. TNFRSF1A mutations and autoinflammatory syndromes. Curr Opin Immunol 2000; 12: 479–486.
8. Kanazawa N, Furukawa F. Autoinflammatory syndromes with a dermatological perspective. J Dermatol 2007: 34: 601–618.
9. Agostini L, Martinon F, Burns K, McDermott MF, Hawkins PN, Tschopp J. NALP3 forms an IL-1beta-processing inflammasome with increased activity in Muckle-Wells autoinflammatory disorder. Immunity 2004; 20: 319–325.
10. Church LD, Cook GP, McDermott MF. Primer: inflammasomes and interleukin 1beta in inflammatory disorders. Nat Clin Pract Rheumatol 2008; 4: 34–42.
11. Martinon F, Burns K, Tschopp J. The inflammasome: a molecular platform triggering activation of inflammatory caspases and processing of proIL-beta. Mol Cell 2002; 10: 417–426.
12. Martinon F, Mayor A, Tschopp J. The inflammasomes: guardians of the body. Ann Rev Immunol 2009; 27: 229–265.
13. Martinon F, Tschopp J. Inflammatory caspases and inflammasomes: master switches of inflammation. Cell Death Differ 2007: 14: 10–22.
14. Pétrilli V, Dostert C, Muruve DA, Tschopp J. The inflammasome: a danger sensing complex triggering innate immunity. Curr Opin Immunol 2007; 19: 615–622.
15. Nakamura Y, Kambe N, Saito M, Nishikomori R, Kim YG, Murakami M, et al. Mast cells mediate neutrophil recruitment and vascular leakage through the NLRP3 inflammasome in histamine-independent urticaria. J Exp Med 2009; 206: 1037–1046.
16. Tamaki K, Yoshida J, Nakabayashi Y. Muckle-Wells syndrome. Hifuka no Rinsyo 1976; 18: 293–303.
17. Yamashita N, Kawakami S, Hidano A, Ohsawa M. Familial cold urticaria. Hifuka no Rinsyo 1987; 29: 1249–1255.
18. Inamo Y, Kin H, Fujita Y, Ochiai T, Okuni M. Chronic, infantile, neurological, cutaneous and articular syndrome in Japan; two case reports. Clin Exp Rheumatol 1994; 12: 447–449.
19. Miura M, Okabe T, Tsubata S, Takizawa N, Sawaguchi T. Chronic infantile neurological cutaneous articular syndrome in a patient from Japan. Eur J Pediatr 1997; 156: 624–626.
20. Mori J, Iehara T, Izumi M, Kato R, Nakajima H, Kizaki Z, et al. A case of chronic infantile neurological cutaneous articular (CINCA) syndrome with marked growth disturbance. Clin Pediatr Endocrinol 2002; 11 Suppl 17: 53–55.
21. Saito M, Fujisawa A, Nishikomori R, Kambe N, Nakata-Hizume M, Yoshimoto M, et al. Somatic Mosaicism of CIAS1 in a patient with chronic infantile neurologic cutaneous articular syndrome. Arthritis Rheum 2005; 52: 3579–3585.
22. Gotoh M, Sonoda K, Ishibashi T, Takada H, Hara T. Uveitis in neonatal onset multisystem inflammatory disease (NOMID). Jap J Clin Ophthalmol 2006; 100: 327–329.
23. Matsubara T, Hasegawa M, Shiraishi M, Hoffman HM, Ichiyama T, Tanaka T, et al. A severe case of chronic infantile neurologic, cutaneous, articular syndrome treated with biologic agents. Arthritis Rheum 2006; 54: 2314–2320.
24. Koike R, Kubota T, Hara Y, Ito S, Suzuki K, Yanagisawa K, et al. A case of Muckle-Wells syndrome caused by a novel

H312P mutation in NALP3 (cryopyrin). Mod Rheumatol 2007; 17: 496–499.
25. Fujisawa A, Kambe N, Saito M, Nishikomori R, Heike T, Miyachi Y. A family case of Cryopyrin-associated Periodic Syndrome. Jpn J Dermatol 2007; 117: 1445–1450.
26. Kawashima H, Sato A, Nishimata S, Yamada N, Kashiwagi Y, Watanabe K, et al. A case report of neonatal onset multisystemic inflammatory disease in Japan treated with continuous hemodiafiltration and steroid pulse therapy. Ther Apher Dial 2007; 11: 232–234.
27. Itazawa T, Kanegane H, Adachi Y, Miyawaki T, Makino T, Shimizu T, et al. A case of familial cold autoinflammatory syndrome. The Allergy in Practice 2008; 28: 221–225.
28. Miyamae T, Inaba Y, Nishimura G, Kikuchi M, Kishi T, Hara R, et al. Effect of anakinra on arthropathy in CINCA/NOMID syndrome. Pediatr Rheumatol Online J 2010; 16: 8–9.
29. Yamauchi A, Iwata H, Ohnishi H, Teramoto T, Kondo N, Seishima M. Interleukin-17 expression in the urticarial rash of familial cold autoinflammatory syndrome: a case report. Br J Dermatol 2010; 163: 1351–1353.

J Clin Immunol
DOI 10.1007/s10875-012-9684-1

Multiple Reversions of an IL2RG Mutation Restore T cell Function in an X-linked Severe Combined Immunodeficiency Patient

Tomoki Kawai · Megumu Saito · Ryuta Nishikomori · Takahiro Yasumi · Kazushi Izawa · Tomohiko Murakami · Shigefumi Okamoto · Yasuko Mori · Noriko Nakagawa · Kohsuke Imai · Shigeaki Nonoyama · Taizo Wada · Akihiro Yachie · Katsuyuki Ohmori · Tatsutoshi Nakahata · Toshio Heike

Received: 7 October 2011 / Accepted: 11 March 2012

Abstract Reversion mosaicism is increasingly being reported in primary immunodeficiency diseases, but there have been few cases with clinically improved immune function. Here, a case is reported of X-linked severe combined immunodeficiency (SCID-X1) with multiple somatic reversions in T cells, which restored sufficient cell-mediated immunity to overcome viral infection. Lineage-specific analysis revealed multiple reversions in T cell receptor (TCR) αβ+ and TCRγδ+ T cells. Diversity of the TCRVβ repertoire was comparable to normal and, furthermore, mitogen-induced

T. Kawai · R. Nishikomori (✉) · T. Yasumi · K. Izawa · T. Heike
Department of Pediatrics,
Kyoto University Graduate School of Medicine,
54 Kawahara-cho, ShogoinSakyo-ku Kyoto 606-8507, Japan
e-mail: rnishiko@kuhp.kyoto-u.ac.jp

T. Kawai
e-mail: tom0818@kuhp.kyoto-u.ac.jp

T. Yasumi
e-mail: yasumi@kuhp.kyoto-u.ac.jp

K. Izawa
e-mail: kizawa@kuhp.kyoto-u.ac.jp

T. Heike
e-mail: heike@kuhp.kyoto-u.ac.jp

M. Saito · T. Nakahata
Clinical Application Department, Center for iPS Cell Research and Application, Institute for Integrated Cell-material Sciences,
Kyoto University,
Kyoto, Japan

M. Saito
e-mail: msaito@kuhp.kyoto-u.ac.jp

T. Nakahata
e-mail: tnakaha@kuhp.kyoto-u.ac.jp

T. Murakami
Kawakita General Hospital,
Tokyo, Japan
e-mail: xyrxf469@ybb.ne.jp

S. Okamoto
Laboratory of Virology and Vaccinology,
Division of Biomedical Research,
National Institute of Biomedical Innovation,
Osaka, Japan
e-mail: sokamoto@nibio.go.jp

Y. Mori
Division of Clinical Virology,
Kobe University Graduate School of Medicine,
Kobe, Japan
e-mail: ymori@med.kobe-u.ac.jp

N. Nakagawa
Department of Pediatrics,
Japan Self Defense Force Hospital Fukuoka,
Kasuga, Japan
e-mail: shikinori@hotmail.com

K. Imai
Department of Developmental Biology and Pediatrics,
Tokyo Medical and Dental University Graduate School of Medical and Dental Sciences,
Saitama, Japan
e-mail: kimai.ped@tmd.ac.jp

S. Nonoyama
Department of Pediatrics,
National Defense Medical College,
Saitama, Japan
e-mail: nonoyama@ndmc.ac.jp

Published online: 30 March 2012

proliferation of the patient's T cells was minimally impaired compared to healthy controls. *In vivo* and *in vitro* varicella antigen-specific T cell responses were comparable to those of healthy controls, although a reduced level of T cell receptor excision circles suggested that recent thymic output was low. During long-term evaluation of the patient's immunologic status, both the number of CD4+ and CD8+ T cells and T cell proliferation responses were stable and the patient remained healthy. This case demonstrates that multiple but restricted somatic reversions in T cell progenitors can improve the clinical phenotype of SCID-X1.

Keywords Severe combined immunodeficiency · reversion · multiple

Introduction

X-linked severe combined immunodeficiency (SCID-X1) is a recessive hereditary disease characterized by a lack of T cells and natural killer (NK) cells. Without stem cell transplantation, persistent infections with opportunistic organisms uniformly lead to death in the first 2 years of life, except in those with atypically attenuated phenotypes [1–3]. Recently, spontaneous genetic reversion has been reported in primary immunodeficiency disorders. Somatic reversion mosaicism is considered to be 'natural gene therapy'; however, few cases are reported with reversions that restore functional immunity [4–9]. Here, an atypical case of SCID-X1 with somatic mosaicism due to multiple reversions in T cells, which restored sufficient T cell immunity, is described.

Materials and Methods

Patient

A male infant was born prematurely at 34 weeks and 4 days of gestation with a birth weight of 1,660 g to healthy parents. There was no family history of consanguinity or immunodeficiency. He was well until 14 months of age, when he started to have recurrent bacterial respiratory tract infections. At the age of 21 months, laboratory tests were performed. Patient results were compared to age-matched normal controls (controls). Examination of serum Ig revealed a decreased level of IgG (IgG, 1.93 g/L [range of controls: 7.15–9.07 g/L]), and normal levels of IgA (IgA, 0.33 g/L [range of controls: 0.22–1.44 g/L]) and IgM (IgM, 0.72 g/L [range of controls: 0.34–1.28 g/L]). His serum IgG was constantly under 2.0 g/L. In addition, he had a reduced number of CD4+ cells (358/μl, [mean of controls: 1,683± 874]) and CD56+ cells (39/μl [mean of controls: 306± 207]), while CD3+ cells (1,803/μl [mean of controls: 2,997±1,751]), CD8+ cells (1,067/μl [mean of controls: 1,683±874]) and CD19+ cells (1,850/μl [mean of controls: 1,114±976]) were within the normal limits. The patient's T cell proliferative response to phytohemagglutinin (PHA) (stimulation index (S.I.) of 172 [range of controls: 105–225]) and to concanavalin-A (Con-A) (S.I. of 140 [range of controls: 68–154]) was within the normal ranges for his age. From these data, he was diagnosed with common variable immunodeficiency (CVID) at that time. Intravenous immunoglobulin therapy was started and he remained in good health thereafter. Without receiving vaccination, varicella infection at 5 years of age did not cause fever, and he was successfully treated with oral acyclovir at an outpatient clinic. At 9 years of age, warts developed and spread over his body, and he was referred to our hospital for assessment of his immunological status. Physical examination revealed neither detectable lymph nodes nor tonsils, and his thymus appeared hypoplastic on CT scan. Before the laboratory studies were performed, informed consent was obtained from the patient and his parents, in accordance with the institutional review board of Kyoto University Hospital and the Declaration of Helsinki.

Flow Cytometry

Flow cytometric analysis was performed according to standard protocols with a FACSCalibur flow cytometer (Becton Dickinson, USA). The following fluorochrome-conjugated antibodies (Abs) were used for flow cytometric analysis: CD3 (clone SK7), CD4 (clone CK3), CD8 (clone SK1), CD14 (clone M5E2), CD19 (clone SJ25C1), CD56 (clone B159), CD45RA (clone HI100), CD45RO (clone UCHL1) (BD Biosciences Pharmingen, USA), TCRαβ (clone IP26A), TCRγδ (clone IMMU 510) (Beckman Coulter, Inc., USA), CCR7 (clone 150503, R&D Systems Inc., USA), CD27 (clone O323, eBioscience, Inc., USA), CD132 (clone TUGh4, BD Biosciences Pharmingen), and rabbit anti-Human IgD polyclonal Ab (DAKO Japan Co., Japan).

T. Wada · A. Yachie
Department of Pediatrics, Graduate School of Medical Science, Kanazawa University,
Kanazawa, Japan

T. Wada
e-mail: taizo@staff.kanazawa-u.ac.jp

A. Yachie
e-mail: yachie@staff.kanazawa-u.ac.jp

K. Ohmori
Department of Laboratory Medicine,
Graduate School of Medicine, Kyoto University,
Kyoto, Japan
e-mail: ohmori@kuhp.kyoto-u.ac.jp

Sequencing of Genomic DNA and cDNA, and Subcloning Analysis

Peripheral blood mononuclear cells (PBMCs) were obtained from the patient and his parents and various cell lineages were sorted using a FACSVantage (Becton Dickinson). The genomic DNA was isolated from the sorted samples and the cDNA was obtained using reverse transcriptase Super Script II (Invitrogen, USA) with Oligo $(dT)_{20}$ primer. Genomic DNA and cDNA were amplified with the proofreading PCR enzyme, KOD –Plus– (Toyobo, Japan). Direct sequencing analysis of all exons of the *IL2RG* gene, including introns at least 50 bases adjacent, were performed on an ABI 3700 (Applied Biosystems, USA). For analysing revertant subclones in each PBMC lineage, the genomic DNA and the cDNA isolated from sorted cell fractions were amplified by PCR with primer pairs 5′-TCCCAGAGGTT CAGTGTTTTG-3′ and 5′-TTGCAACTGACAGCCA GAAG-3′, and 5′-CGCCATGTTGAAGCCATC-3′ and 5′-TTGCAACTGACAGCCAGAAG-3′, for the region spanning exons 2 and 3 of *IL2RG,* respectively. These PCR products were subcloned using a TOPO TA Cloning Kit (Invitrogen) and sequenced.

T cell Functional Assays

To obtain PHA-induced T cell blasts, PBMCs were stimulated with PHA (Invitrogen) at 1:100 dilution and cultured in RPMI 1640 (RPMI) supplemented with 5 % fetal calf serum (FCS) with recombinant human IL-2 (50 IU/ml, kindly provided by Takeda Pharmaceutical Company, Japan) at 37 °C for 7 days. After being rested in RPMI with 5 % FCS overnight, the T cell blasts were stimulated with various concentrations of IL-2 for 48 h, and [^{3}H]-thymidine uptake assays were performed as previously described [8]. T cell receptor (TCR) Vβ repertoire analysis and CDR3 spectratyping were performed as described [10, 11]. *In vitro* cytokine production against varicella zoster virus (VZV) antigen was performed as previously described [12]. Spots were enumerated automatically using the KS ELISPOT system (Carl Zeiss). The *in vivo* delayed-type hypersensitivity (DTH) reaction to subcutaneous purified VZV antigen (BIKEN, Japan) was performed as previously described [13]. The T cell receptor excision circles (TRECs) from the patient PBMCs were measured as previously described [14].

Tyrosine Phosphorylation of STAT5 by IL-2

PBMCs (1×10^6) were cultured in RPMI with 5 % FCS at 37 °C for 2 h and then treated with or without IL-2 (10,000 U/ml) for 10 min. The cells were fixed and permeabilized with BD Cytofix Buffer and Phosflow Perm Buffer III (BD Biosciences Pharmingen) according to the manufacturer's instructions. After washing with PBS containing 1 % FCS, the cells were stained with mouse anti-pSTAT5 (pY694) (clone 47, BD biosciences), anti-CD4 and anti-CD8 mAbs and analyzed by flow cytometry.

Results and Discussion

At the age of 9 years, the patient presented with generalized warts and no detectable lymph nodes and tonsils. This, coupled with his prior hypogammaglobulinemia, prompted a re-evaluation of his immunological status. He showed a decreased level of IgA and a normal level of IgM but no isohemagglutinin. Mitogen-induced proliferation assays showed a slightly reduced response to PHA and Con A (Table I). Surface marker analysis of PBMCs revealed slightly decreased levels of CD3+ and CD4+ T cells, and a normal level of CD8+ T cells (Table II). Naïve CD4+ T cells

Table I Laboratory investigations (patient aged 9 years)

		Patient (IVIG)	Healthy controls
Blood counts			
White blood cells	(count/μl)	7,400	3,600–9,800
Neutrophil	(count/μl)	4,773	3,000–5,000
Lymphocyte	(count/μl)	2,028	2,500–4,500
Monocyte	(count/μl)	340	200–950
Eosinophil	(count/μl)	252	0–700
Basophil	(count/μl)	7	0–150
Red blood cells	($\times10^6$ count/μl)	5.15	4.08–5.07
Hemoglobin	(g/dl)	12.5	11.6–14.1
Platelet	($\times10^3$ count/μl)	275	201–409
Serum Immunoglobulin levels			
IgG	(g/L)	7.69	10.79±2.63
IgA	(g/L)	0.26	2.46±0.91
IgM	(g/L)	1.08	0.83±0.21
IgD	(mg/L)	<6	55±16
IgE	(IU/mL)	<5	<170
isohemagluttinin		Undetectable	
T cell proliferation			
None	(cpm)	163	127–456
Phytohemagglutinin	(cpm)	16,800	20,500–56,800
Concanavalin A	(cpm)	16,600	20,300–65,700
DTH reaction to subcutaneous varicella virus antigen			
Erythematous change (mm in diameter)		18	≧5.0

Control values of blood counts are shown as the range from 95 % of healthy children aged 9 to 12 years. Control values of serum immunoglobulin levels are based on children aged 8 to 10 years and are shown as the mean ± SD. IVIG indicates monthly intravenous infusion of 2.5 g immunoglobulin

Table II Surface marker analysis of peripheral blood mononuclear cells (patient aged 9 years)

	Patient (count/μl)	Healthy controls (count/μl)
CD3+	1,080	2,813±1,197
CD4+	357	1,699±850
CD8+	582	972±457
TCRαβ+	890	2,154±1,004
TCRγδ+	190	324±182
CD4+CD45RA+CCR7+	8	1,290±756
CD8+CD45RA+CCR7+	25	655±503
CD8+CD45RA+CCR7-	114	221±95.3
CD8+CD45RA-CCR7+	33	30.1±27.6
CD8+CD45RA-CCR7-	410	132±87.4
CD19+	894	1,238±605
CD19+CD27+smIgD-	0.4	86.6±61.3
CD19+CD27+smIgD+	14.3	172±123
CD3-CD56+	Undetectable	271±186

Absolute numbers of cells expressing surface markers are shown. Healthy control values are from children aged 2 to 9 years and are shown as mean ± SD

(CD4+/CD45RA+/CCR7+), naïve CD8+ T cells (CD8+/CD45RA+/CCR7+), and both switched memory B cells (CD19+/CD27+/smIgD-) and unswitched memory B cells (CD19+/CD27+/cmIgD-) were scarce. In addition, natural killer (NK) cells (CD3-/CD56+) were absent. This suggested the existence of a genetic defect causing lack of NK cells, such as an *IL2RG* deficiency and *JAK3* deficiency, and therefore the expression of IL2RG (also known as the common gamma chain or CD132) was examined by flow cytometry. Reduced expression was found on B cells and monocytes, although T cells expressed normal levels of CD132 (Fig. 1a). To determine whether CD132-dependent signal transduction was functioning, STAT5 phosphorylation was analyzed on patient CD4+ and CD8+ T cells in response to IL-2. It was found to be comparable with that of normal controls (Fig. 1b). In addition, a proliferation assay of PHA-induced T cell blasts in response to exogenous IL-2 was performed (Fig. 1c). This confirmed that the patient T cells, which were expressing normal levels of CD132, also had intact IL-2 signaling.

To elucidate the genetic cause of the lineage-dependent CD132 expression abnormalities, *IL2RG* genomic sequencing was performed in various cell lineages. Genomic sequencing of *IL2RG* in B cells, monocytes and buccal mucosa revealed a point mutation, c.284-15A>G, in intron 2 of *IL2RG*. This has been reported as a causative mutation of SCID-X1 [15], producing aberrant mRNA with an insertion of 14 bases spanning nucleotide −14 to −1 of exon 3 (Fig. 2a, b). Genomic sequencing of *IL2RG* in T cells showed overlapping bases at and around the mutation sites, while the cDNA of *IL2RG* from

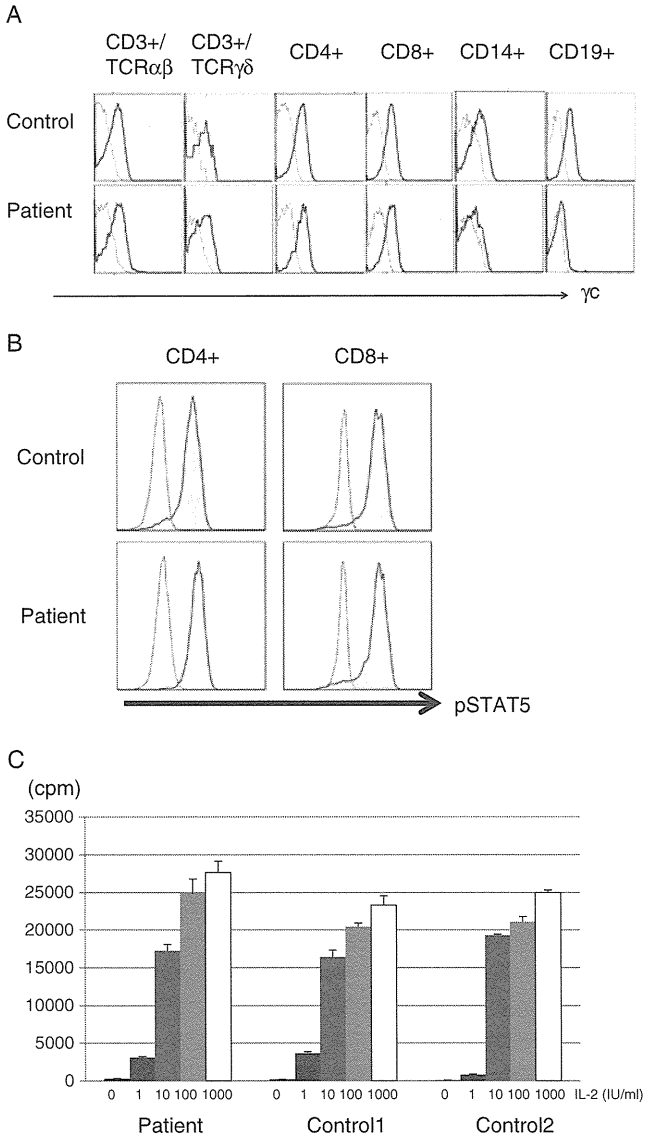

Fig. 1 IL2RG expression and T cell function at 9 years old. **a** Surface expression of IL2RG on PBMCs from the patient and healthy control gated according to the expression of the indicated lineage surface markers. *Black lines* indicate staining for IL2RG (with anti-CD132 Ab) and *gray lines* indicate staining with the isotype control. Data represent one of three independent experiments. **b** STAT5 tyrosine phosphorylation in patient and control CD4+ and CD8+ cells after incubation with (*shaded histograms*) or without IL-2 (*open histograms*). **c** Proliferation of PHA-induced T cell blasts in response to IL-2 stimulation from the patient and two controls. Data are shown as means ± SD

the T cells was normal (Fig. 2a, b). Genomic sequencing of PBMCs from the patient's mother confirmed her as a carrier of the mutation. The possibility of maternal engraftment was excluded by FISH analysis of sex chromosomes (data not shown), and it was concluded that the patient inherited the mutation from his mother and that reversion occurred in the patient's T cells, which led to somatic mosaicism.

To explore the reversions that could have occurred to restore normal *IL2RG* expression in the patient's T cells,

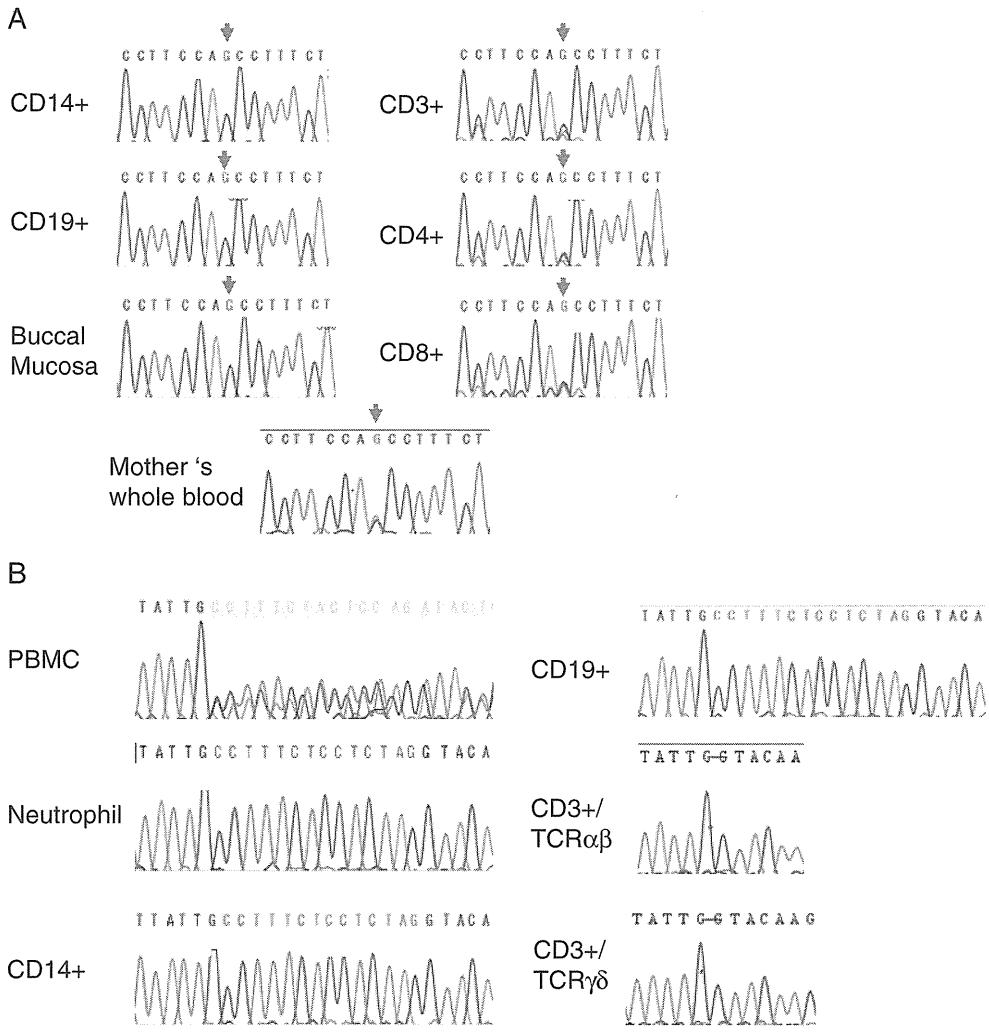

Fig. 2 Genetic analysis of various cell lineages at 9 years old. **a** Sequencing chromatograms of the patient's DNA from various immune cell lineages and buccal mucosa. *Red arrows* indicate the mutated base position c. 284–15. PBMCs from the patient's mother carried the same mutation. The patient's T cells show overlapping base changes at or around the mutated site. Data represent one of three independent experiments. **b** Sequencing chromatograms of the patient's cDNA from various cell types. Re characters indicate the inserted 14 bases spanning nucleotide −14 to nucleotide −1 of exon 3

subcloning and sequencing analysis of genomic DNA and cDNA was performed in various cell lineages. In B cells and monocytes, no reversion was detected and all of the cDNA clones had aberrant splicing (Table III). Analysis of TCRαβ+ cells revealed seven reversions, a true-back reversion, two fully compensating same-site reversions and four second-site reversions, all of which favored a functional reversion according to the splicing analysis software NNSPLICE0.9 [16] (Table IV). None of these base changes were detected in 200 clones from four healthy controls, indicating that the identified intron changes were unlikely to be due to PCR errors. The multiple reversions seen in this case differed from the single reversions seen in other reported cases of reversion mosaicism of SCID-X1 [2, 3]. One possible reason for this is that, compared with the previously reported exonic mutations, an intronic mutation is more likely to acquire additional reversions on top of a true-back mutation. Additionally, the nine-year lifespan of the patient may have provided increased opportunities for extra reversions to occur. TCRVβ V-to-DJ rearrangement is reported to be impaired in some SCID-X1 patients, suggesting that differentiation arrest occurs at the CD4 immature single positive (ISP) stage at which TCRVβ V-to-DJ recombination is completed in normal T cells [17]. Therefore, the

Table III Clonal analysis of *IL2RG* cDNA in various cell lineages

	CD3+	CD4+	CD8+	CD14+	CD19+
Wild-type cDNA	100 % (25/25)	100 % (31/31)	100 % (30/30)	0 % (0/45)	0 % (0/34)
Aberrant cDNA	0 % (0/25)	0 % (0/31)	0 % (0/30)	100 % (45/45)	100 % (34/34)

Data represent the percentages of wild-type or aberrant spliced cDNA subclones in each lineage. The ratio indicates the number of each clone as compared to the total number of clones analyzed, based on subcloning and sequencing analysis

Table IV Multiple additional mutations detected in subclones of the *IL2RG* gene

	Subclones	Mutations
Wild type	TT CCTCT T CCT T CCAACC	Wild type
Inherited mutation	TT CCTCT T CCT T CCAGCC	c.284-15A>G
No.1	TT CCTCT T CCT T CCATCC	c.284-15A>T
No.2	TT CCTCT T CCT T CCACCC	c.284-15A>C
No.3	TT CCTCT T CAT T CCAGCC	c.284-15A>G, c.284-21C>A
No.4	TT AGAGTGG CCTCT T CCT T CCAGCC	c.284-15A>G, c.284-29_284-28insAGAGTGG
No.5	TT CCTC CACCCGCCAAC	c.284-24_284-14del11ins CACCCGCCAA
No.6	TT CCTCT CAGCC	c.284-23_284-18delTCCTTC

reversions found in the patient's T cells must have occurred before or around the CD4ISP stage. Differences were observed in reversion genotypes between the TCRαβ+ cells and TCRγδ+ cells. TCRγδ+ cells had only one of the second-site reversions found in TCRαβ+ cells in addition to a true-back reversion (No.3 in Table V). The identification of fewer reversions in the patient's TCRγδ+ compared to TCRαβ+ cells may reflect the greater abundance of TCRαβ+ cells, increasing the likelihood of the stochastic occurrence of additional reversions [18]. Although no reversions in the patient's B cells or monocytes were observed, it is possible that the reversions occurred in the progenitor at the stage before commitment to T cells and may reflect the unique nature of T cell proliferation and expansion [19].

Reversion mosaicism has previously been reported in SCID-X1 patients with *IL2RG* mutations, but it was accompanied by reduced T cell number and low proliferative response to mitogens [2, 3]. The paradoxical nature of the patient's cellular immunity, a history of uneventful varicella infection, and the occurrence of widespread warts with very few naïve T cells prompted an evaluation of his T cell function. The TCR Vβ repertoire analysis of CD4+ and CD8+ T cells revealed comparable diversity to the normal controls (data not shown). CDR3 spectratyping analysis revealed the patient CD4+ T cells had as much variety as the normal controls, but his CD8+ T cells displayed restricted diversity (Fig. 3a). To evaluate the antigen-specific response of the patient's T cells, response to VZV was measured. The DTH reaction to subcutaneous VZV antigen and the IFN-γ production from VZV antigen-stimulated PBMCs measured by an ELISPOT assay were comparable to those of normal controls (Table I and Fig. 3b). These data suggested that the patient maintained normal cellular immune responses *in vivo* as well as having normal *in vitro* IFN-γ production ability against VZV antigen. Multiple reversions from intronic mutations could provide a sufficient number of normally functioning T cells and may improve the clinical phenotype compared to previously reported cases with single reversions. However, the number of TRECs in the patient's PBMCs (<10 copies/μg DNA) suggested a low level of recent thymic output, and the restricted diversity of TCRs observed in the patient's CD8+ cells might reflect the exhaustion of the T cell reservoir. To gain further insight, the long-term immunologic status of the patient was evaluated prospectively for 5 years. Absolute counts of CD4+ and CD8+ T cells as well as mitogen-induced T cell proliferation responses were measured every 2–5 months (Fig. 4). Unexpectedly, the number of both CD4+ and CD8+ T cells and mitogen-induced T cell proliferation responses were stable and the patient remained healthy over this period. In recent years, the effector memory subset of CD8+ T cells (CD8+/CD45RA+/CCR7-) has been taken as a marker of cell exhaustion or replicative senescence [20]. However, the majority of CD8+ T cells of the patient were memory CD8+ T cells (CD8+/CD45RA-/CCR7±) and the population of effector memory CD8+ T cells was very small (Table II). These data

Table V Clonal analysis of somatic mosaicism of the *IL2RG* gene in various cell lineages

	Wild type	Inherited mutation	No.1	No.2	No.3	No.4	No.5	No.6
TCRαβ+	21 % (7/33)	12 % (4/33)	9 % (3/33)	12 % (4/33)	21 % (7/33)	9 % (3/33)	6 % (2/33)	9 % (3/33)
TCRγδ+	2 % (1/42)	2 % (1/42)	0 % (0/42)	0 % (0/42)	95 % (40/42)	0 % (0/42)	0 % (0/42)	0 % (0/42)
CD3+	5 % (2/39)	5 % (2/39)	26 % (10/39)	13 % (5/39)	38 % (15/39)	3 % (1/39)	10 % (4/39)	0 % (0/39)
CD4+	32 % (25/79)	3 % (2/79)	13 % (10/79)	19 % (15/79)	16 % (13/79)	3 % (2/79)	3 % (2/79)	13 % (10/79)
CD8+	10 % (7/73)	4 % (3/73)	21 % (15/73)	19 % (14/73)	25 % (18/73)	8 % (6/73)	12 % (9/73)	1 % (1/73)
CD14+	0 % (0/33)	100 % (33/33)	0 % (0/33)	0 % (0/33)	0 % (0/33)	0 % (0/33)	0 % (0/33)	0 % (0/33)
CD19+	0 % (0/30)	100 % (30/30)	0 % (0/30)	0 % (0/30)	0 % (0/30)	0 % (0/30)	0 % (0/30)	0 % (0/30)

Data represent the percentages of each additional mutant subclone in each lineage. The ratio indicates the number of each mutant clone in various cell lineages as compared to the total number of clones analyzed, based on subcloning and sequencing analysis

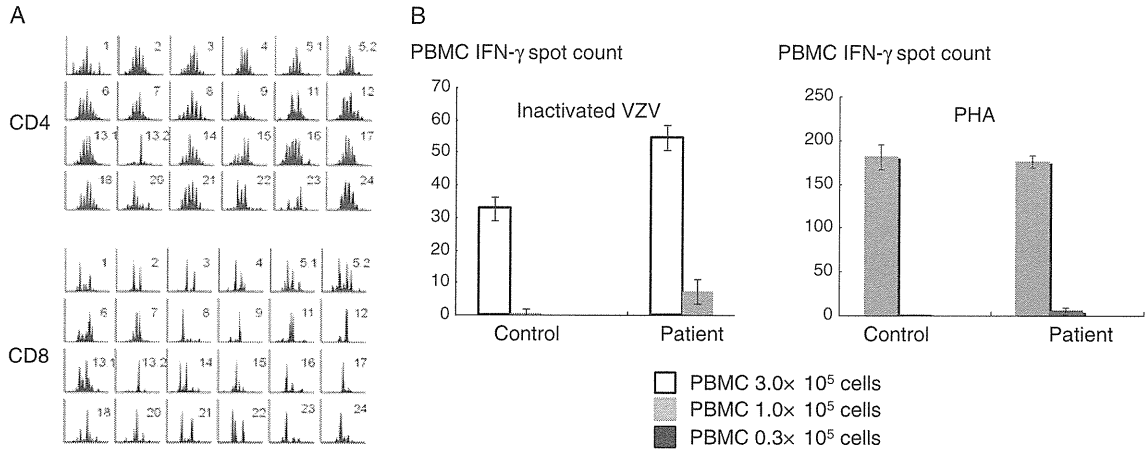

Fig. 3 Functional evaluation of T cells at 9 years old. **a** CDR3 spectratyping of the TCRVβ chain. Each TCRVβ fragment was amplified from cDNA with one of 24Vβ-specific primers (each Vβ chain is indicated). The size distribution of the PCR products was determined by an automated sequencer and GeneScan software. The CDR3 size distribution in CD4+ and CD8+ T cells from the patient is shown. **b** Elispot analysis of IFN-γ production as a measure of T cell function. (LEFT) Varicella-specific immune response to varicella zoster (VZV) antigen *in vitro*. Patient and control (from a healthy with a previous history of varicella infection) PBMCs ($0.3\text{-}3\times10^5$) were stimulated with inactivated VZV antigen or (RIGHT) PHA. Data are shown as mean ± SD

demonstrated that the patient maintained a certain level of T cell immunity for over a decade, despite the fact that the supply of fresh T cells from the thymus was limited and the patient suffered from generalized warts. Further follow up is required to determine if the patient can continue to maintain long-term T cell immunity.

In conclusion, this study indicates that it is critical to determine the NK cell number to avoid overlooking reversion mosaicism of SCID-X1. In addition, it has been shown that a number of *IL2RG* gene reversions can restore T cell functions and maintain T cell immunity against viral infection for at least 14 years.

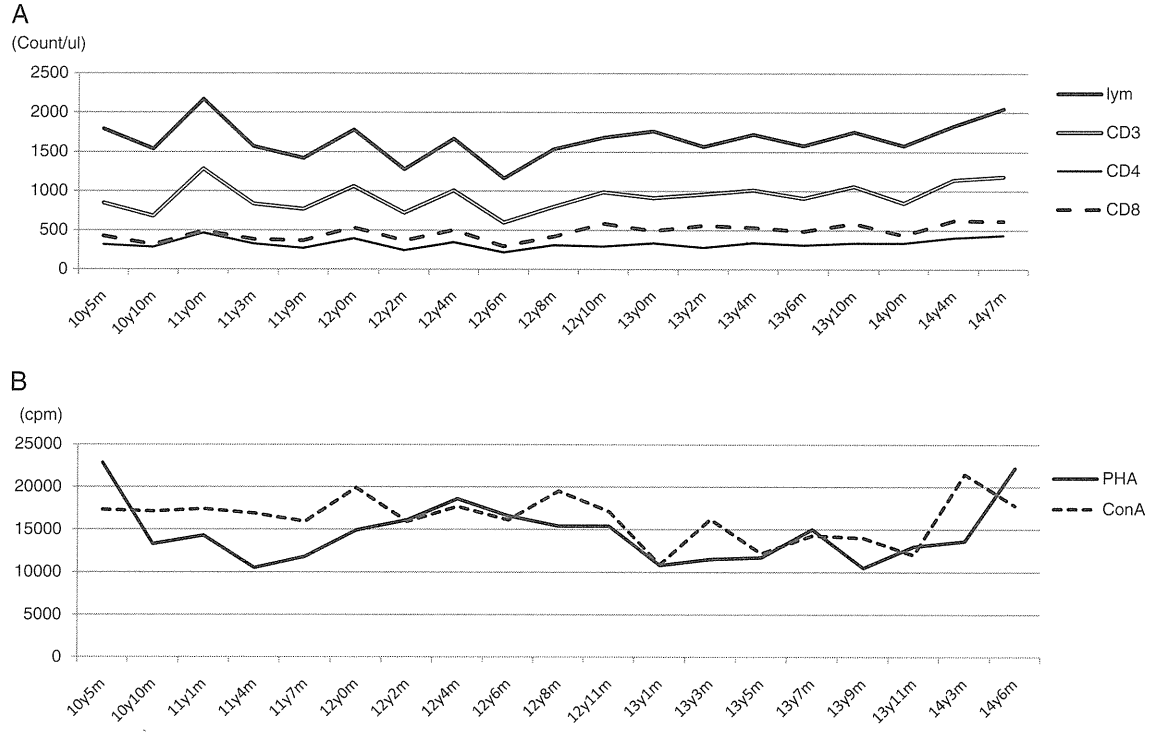

Fig. 4 Long term evaluation of T cell number and mitogen-induced proliferative response. **a** Absolute counts (per μl) of total lymphocytes (lym), CD3+ cells, CD4+ cells and CD8+ cells were measured for 4 years. **b** T cell proliferation in response to PHA (*solid line*) and Con A (*dotted line*). Healthy control values for PHA range from 20,500 to 56,800 cpm and for Con A from 20,500 to 65,700 cpm

Acknowledgements We are grateful to the patient and his family for their participation. We also thank Takeda Pharmaceutical Company (Osaka, Japan) for kindly providing recombinant IL-2.

Authors' contributions T.K. performed experiments and wrote the paper. M.S. and Ka.I. performed experiments. R.N. designed the research, wrote the paper and analyzed data. Y.T. wrote the paper and analyzed data. T.M. treated the patient and analyzed data. S.O., Y.M., N.N., Ko.I, S.N., T.W. and A.Y. performed experiments and discussed the research. T.H. and T.N. designed the research.

Conflict of Interests The authors declare no competing financial interests.

References

1. Buckley RH. Primary immunodeficiency diseases: dissectors of the immune system. Immunol Rev. 2002;185:206–19.
2. Stephan V, Wahn V, Le Deist F, Dirksen U, Broker B, Muller-Fleckenstein I, et al. Atypical X-linked severe combined immunodeficiency due to possible spontaneous reversion of the genetic defect in T cells. N Engl J Med. 1996;335(21):1563–7.
3. Speckmann C, Pannicke U, Wiech E, Schwarz K, Fisch P, Friedrich W, et al. Clinical and immunologic consequences of a somatic reversion in a patient with X-linked severe combined immunodeficiency. Blood. 2008;112(10):4090–7.
4. Hirschhorn R, Yang DR, Puck JM, Huie ML, Jiang CK, Kurlandsky LE. Spontaneous in vivo reversion to normal of an inherited mutation in a patient with adenosine deaminase deficiency. Nat Genet. 1996;13(3):290–5.
5. Hirschhorn R. In vivo reversion to normal of inherited mutations in humans. J Med Genet. 2003;40(10):721–8.
6. Ariga T, Kondoh T, Yamaguchi K, Yamada M, Sasaki S, Nelson DL, et al. Spontaneous in vivo reversion of an inherited mutation in the Wiskott-Aldrich syndrome. J Immunol. 2001;166(8):5245–9.
7. Wada T, Toma T, Okamoto H, Kasahara Y, Koizumi S, Agematsu K, et al. Oligoclonal expansion of T lymphocytes with multiple second-site mutations leads to Omenn syndrome in a patient with RAG1-deficient severe combined immunodeficiency. Blood. 2005;106(6):2099–101.
8. Nishikomori R, Akutagawa H, Maruyama K, Nakata-Hizume M, Ohmori K, Mizuno K, et al. X-linked ectodermal dysplasia and immunodeficiency caused by reversion mosaicism of NEMO reveals a critical role for NEMO in human T-cell development and/or survival. Blood. 2004;103(12):4565–72.
9. Uzel G, Tng E, Rosenzweig SD, Hsu AP, Shaw JM, Horwitz ME, et al. Reversion mutations in patients with leukocyte adhesion deficiency type-1 (LAD-1). Blood. 2008;111(1):209–18.
10. Ariga T, Oda N, Yamaguchi K, Kawamura N, Kikuta H, Taniuchi S, et al. T-cell lines from 2 patients with adenosine deaminase (ADA) deficiency showed the restoration of ADA activity resulted from the reversion of an inherited mutation. Blood. 2001;97(9):2896–9.
11. Konno A, Okada K, Mizuno K, Nishida M, Nagaoki S, Toma T, et al. CD8alpha alpha memory effector T cells descend directly from clonally expanded CD8alpha+ beta high TCRalpha beta T cells in vivo. Blood. 2002;100(12):4090–7.
12. Sadaoka K, Okamoto S, Gomi Y, Tanimoto T, Ishikawa T, Yoshikawa T, et al. Measurement of varicella-zoster virus (VZV)-specific cell-mediated immunity: comparison between VZV skin test and interferon-gamma enzyme-linked immunospot assay. J Infect Dis. 2008;198(9):1327–33.
13. Kamiya H, Ihara T, Hattori A, Iwasa T, Sakurai M, Izawa T, et al. Diagnostic skin test reactions with varicella virus antigen and clinical application of the test. J Infect Dis. 1977;136(6):784–8.
14. Morinishi Y, Imai K, Nakagawa N, Sato H, Horiuchi K, Ohtsuka Y, et al. Identification of severe combined immunodeficiency by T-cell receptor excision circles quantification using neonatal guthrie cards. J Pediatr. 2009;155(6):829–33.
15. Tassara C, Pepper AE, Puck JM. Intronic point mutation in the IL2RG gene causing X-linked severe combined immunodeficiency. Hum Mol Genet. 1995;4(9):1693–5.
16. Reese MG, Eeckman FH, Kulp D, Haussler D. Improved splice site detection in Genie. J Comput Biol. 1997;4(3):311–23.
17. Sleasman JW, Harville TO, White GB, George JF, Barrett DJ, Goodenow MM. Arrested rearrangement of TCR V beta genes in thymocytes from children with X-linked severe combined immunodeficiency disease. J Immunol. 1994;153(1):442–8.
18. Joachims ML, Chain JL, Hooker SW, Knott-Craig CJ, Thompson LF. Human alpha beta and gamma delta thymocyte development: TCR gene rearrangements, intracellular TCR beta expression, and gamma delta developmental potential–differences between men and mice. J Immunol. 2006;176(3):1543–52.
19. Freitas AA, Rocha B. Population biology of lymphocytes: the flight for survival. Annu Rev Immunol. 2000;18:83–111.
20. Appay V, van Lier RA, Sallusto F, Roederer M. Phenotype and function of human T lymphocyte subsets: consensus and issues. Cytometry A. 2008;73(11):975–83.

blood

2011 118: 1225-1230
Prepublished online June 8, 2011;
doi:10.1182/blood-2011-01-329540

Rapid diagnosis of FHL3 by flow cytometric detection of intraplatelet Munc13-4 protein

Yuuki Murata, Takahiro Yasumi, Ryutaro Shirakawa, Kazushi Izawa, Hidemasa Sakai, Junya Abe, Naoko Tanaka, Tomoki Kawai, Koichi Oshima, Megumu Saito, Ryuta Nishikomori, Osamu Ohara, Eiichi Ishii, Tatsutoshi Nakahata, Hisanori Horiuchi and Toshio Heike

Blood (print ISSN 0006-4971, online ISSN 1528-0020), is published weekly by the American Society of Hematology, 2021 L St, NW, Suite 900, Washington DC 20036.

Rapid diagnosis of FHL3 by flow cytometric detection of intraplatelet Munc13-4 protein

Yuuki Murata,[1] Takahiro Yasumi,[1] Ryutaro Shirakawa,[2] Kazushi Izawa,[1] Hidemasa Sakai,[1] Junya Abe,[1] Naoko Tanaka,[1] Tomoki Kawai,[1] Koichi Oshima,[3-5] Megumu Saito,[3] Ryuta Nishikomori,[1] Osamu Ohara,[4,5] Eiichi Ishii,[6] Tatsutoshi Nakahata,[3] Hisanori Horiuchi,[2] and Toshio Heike[1]

[1]Department of Pediatrics, Kyoto University Graduate School of Medicine, Kyoto, Japan; [2]Department of Molecular and Cellular Biology, Institute of Development, Aging and Cancer, Tohoku University, Sendai, Japan; [3]Clinical Application Department, Center for iPS Cell Research and Application, Kyoto University, Kyoto, Japan; [4]Department of Human Genome Research, KAZUSA DNA Research Institute, Kisarazu, Japan; [5]Laboratory for Immunogenomics, Research Center for Allergy and Immunology, RIKEN, Yokohama, Japan; and [6]Department of Pediatrics, Ehime University Graduate School of Medicine, Toon, Japan

Familial hemophagocytic lymphohistiocytosis (FHL) is a potentially lethal genetic disorder of immune dysregulation that requires prompt and accurate diagnosis to initiate life-saving immunosuppressive therapy and to prepare for hematopoietic stem cell transplantation. In the present study, 85 patients with hemophagocytic lymphohistiocytosis were screened for FHL3 by Western blotting using platelets and by natural killer cell lysosomal exocytosis assay. Six of these patients were diagnosed with FHL3. In the acute disease phase requiring platelet transfusion, it was difficult to diagnose FHL3 by Western blot analysis or by lysosomal exocytosis assay. In contrast, the newly established flow cytometric analysis of intraplatelet Munc13-4 protein expression revealed bimodal populations of normal and Munc13-4–deficient platelets. These findings indicate that flow cytometric detection of intraplatelet Munc13-4 protein is a sensitive and reliable method to rapidly screen for FHL3 with a very small amount of whole blood, even in the acute phase of the disease. (*Blood*. 2011;118(5):1225-1230)

Introduction

The granule-dependent cytotoxic pathway is a major immune effector mechanism used by cytotoxic T lymphocytes (CTLs) and natural killer (NK) cells.[1] The pathway involves a series of steps, including cell activation, polarization of the lysosomal granules to the immunologic synapse, exocytosis of lytic proteins such as perforin and granzymes, and induction of apoptosis in the target cells.[2] In addition to its central role in the defense against intracellular infections and in tumor immunity, this pathway also plays an important role in the regulation of immune homeostasis. Defects in the granule-dependent cytotoxic pathway result in a catastrophic hyperinflammatory condition known as hemophagocytic lymphohistiocytosis (HLH).[1,3]

HLH is a life-threatening syndrome of immune dysregulation resulting from the uncontrolled activation and proliferation of CTLs, which leads to macrophage activation and the excessive release of inflammatory cytokines.[4,5] Clinical diagnosis of HLH is made on the basis of cardinal signs and symptoms including prolonged fever and hepatosplenomegaly, and by characteristic laboratory findings such as pancytopenia, hyperferritinemia, hypofibrinogenemia, increased levels of soluble IL-2 receptor, and low or absent NK cell activity.[5,6] HLH can be classified into primary (genetic) or secondary (acquired) forms according to the underlying etiology, although this distinction is difficult to make in clinical practice.[4,5]

Familial hemophagocytic lymphohistiocytosis (FHL) encompasses major forms of primary HLH for which mutations in the genes encoding perforin (*PRF1*; FHL2),[7] Munc13-4 (*UNC13D*; FHL3),[8] syntaxin-11 (*STX11*; FHL4),[9] and syntaxin-binding protein 2 (also known as Munc18-2) (*STXBP2*; FHL5)[10,11] have been identified to date. Perforin is a cytolytic effector that forms a pore-like structure in the target cell membrane. Munc13-4, syntaxin-11, and Munc18-2 are involved in intracellular trafficking or the fusion of cytolytic granules to the plasma membrane and the subsequent delivery of their contents into target cells.[1,12] Consequently, defective cytotoxic activity of CTLs and NK cells is one of the hallmark findings of FHL,[7,8,13-16] although NK cell activity is also decreased in some cases of secondary HLH.[15,17-20]

Prompt and accurate diagnosis of FHL is mandatory to initiate life-saving immunosuppressive therapy and to prepare for hematopoietic stem cell transplantation. Detection of perforin expression in NK cells with flow cytometry is a reliable method to screen for FHL2.[21] Another test analyzes the expression of CD107a on the surface of NK cells, which marks the release of cytolytic granules.[22] Reduced expression of CD107a implies impaired degranulation of NK cells and predicts a likelihood of FHL3.[23] However, this analysis is not available in some patients with extremely reduced NK cell numbers, such as during the acute phase of HLH.[19] In addition, NK-cell degranulation is also impaired in FHL4[24] and FHL5,[10,11] making it impossible to differentiate these disorders.

We reported previously that Munc13-4 protein is expressed in platelets and regulates the secretion of dense core granules.[25] Herein we report that Munc13-4 is expressed far more abundantly in platelets than in PBMCs. We also describe the development of a

Submitted January 10, 2011; accepted May 23, 2011. Prepublished online as *Blood* First Edition paper, June 8, 2011; DOI 10.1182/blood-2011-01-329540.

The online version of this article contains a data supplement.

The publication costs of this article were defrayed in part by page charge payment. Therefore, and solely to indicate this fact, this article is hereby marked "advertisement" in accordance with 18 USC section 1734.

new method to screen for FHL3 rapidly by detecting intraplatelet Munc13-4 expression through flow cytometry.

Methods

Patients

Between January 2008 and March 2010, whole blood samples from 85 patients were screened for FHL3. The patients had been clinically diagnosed with HLH by their referring physicians and were suspected of possible FHL. Characteristics of the enrolled patients are summarized in supplemental Table 1 (available on the *Blood* Web site; see the Supplemental Materials link at the top of the online article). As a control, blood obtained from healthy adults at the time of patient sampling was shipped for screening along with the patient samples. Before the laboratory studies were performed, informed consent was obtained from the patients and their parents, in accordance with the institutional review board of Kyoto University Hospital and the Declaration of Helsinki.

Preparation of PBMCs and platelet samples

Whole blood samples treated with EDTA were centrifuged gently at 100*g* for 10 minutes, and platelets were collected from the supernatant plasma layer. Alternatively, platelets were prepared from small aliquots of blood samples by lysing red blood cells with ammonium chloride. PBMCs were obtained by Ficoll-Hypaque density gradient centrifugation from the remaining sample. $CD4^+$, $CD8^+$, $CD14^+$, $CD19^+$, and $CD45^+$ cells were separated from PBMCs using an AutoMACS Pro (Miltenyi Biotec) and magnetic bead–conjugated mAbs according to the manufacturer's instructions. Flow cytometric analysis revealed that each cell population contained > 95% $CD4^+$, $CD8^+$, $CD14^+$, $CD19^+$, and $CD45^+$ cells (data not shown).

Mutation analysis

Genomic DNA was isolated from the PBMCs of patients with defective Munc13-4 expression using standard procedures. Primers were designed for the amplification and direct DNA sequencing of the *UNC13D*-coding exons, including the adjacent intronic sequences for the identification of splice-site variants. Primer sequences are available upon request. Products were sequenced directly with an ABI3130 genetic analyzer (Applied Biosystems).

Antibodies

Rabbit polyclonal antibodies raised against the N-terminal region (residues 1-262)[25] and full-length human Munc13-4 protein were used as primary antibodies for Western blot and flow cytometric analysis, respectively. Rabbit polyclonal anti-integrin αIIb (Santa Cruz Biotechnology) and mouse polyclonal anti–β-actin (Sigma-Aldrich) antibodies were used as primary antibodies for Western blotting. The mAbs used in the flow cytometric analysis were FITC-conjugated anti-CD3 (SK7; BD Pharmingen), phycoerythrin (PE)–conjugated anti-CD41a (HIP8; BD Pharmingen); allophycocyanin-conjugated anti-CD56 (N901; Beckman Coulter), and PE-conjugated anti-CD107a (H4A3; eBioscience).

Western blot analysis

Cell extracts were fractionated by SDS-PAGE, and the fractionated proteins were electrotransferred onto polyvinylidene fluoride membranes. The membranes were blocked overnight in blocking buffer (5% skim milk) and incubated for 1 hour at room temperature with the primary antibodies, followed by HRP-conjugated anti–rabbit or anti–mouse IgG polyclonal antibodies (Santa Cruz Biotechnology). Specific bands were visualized by the standard enhanced chemiluminescence method.

Flow cytometric analysis of Munc13-4 protein

After surface staining with anti-CD41a mAbs, platelets were fixed and permeabilized by Cytofix/Cytoperm (BD Biosciences) and washed 3 times with Perm/Wash buffer (BD Biosciences). After nonspecific reactions were blocked with Chrome-Pure human IgG (Jackson ImmunoResearch Laboratories), rabbit polyclonal antibody against the full-length human Munc13-4 protein was added, followed by FITC-conjugated donkey anti–rabbit IgG (Jackson ImmunoResearch Laboratories). Platelets were gated on the basis of their appearance on forward- and side-scatter plots in log/log scale and by CD41a expression. The gated platelets were analyzed for Munc13-4 expression by flow cytometry (FACSCalibur; BD Biosciences).

Lysosomal degranulation assays

To quantify lysosome exocytosis by NK cells, 2×10^5 PBMCs were mixed with 2×10^5 human erythroleukemia cell line K562 cells and incubated for 2 hours in complete medium (RPMI 1640 medium supplemented with 2mM L-glutamine and 10% FCS) at 37°C in 5% CO_2. Cells were resuspended in PBS supplemented with 2% FCS and 2mM EDTA; stained with anti-CD3–FITC, anti-CD56–allophycocyanin, and anti-CD107a–PE mAbs; and analyzed by flow cytometry.

Platelet exocytosis of the lysosomal granules was analyzed as described previously[26] but with a minor modification. Briefly, platelets were suspended in PBS containing 2mM EDTA and PE-conjugated anti-CD107a mAb, stimulated with 5 U/mL of thrombin (Wako Pure Chemical Industries) for 10 minutes at 25°C, and immediately analyzed by flow cytometry. The degranulation index of platelets was calculated as: (mean fluorescence value of stimulated sample − mean fluorescence value of nonstimulated sample)/mean fluorescence value of nonstimulated sample.

Statistical analysis

Statistical analyses were performed with 1-way ANOVA followed by the Tukey post hoc test to compare multiple groups, with a $P < .05$ level considered to be significant.

Results

Diagnosis of FHL3 by Western blot analysis using platelets

Before screening for FHL3, the Munc13-4 expression level was compared between platelets and PBMCs. Munc13-4 expression in platelets was approximately 10 times higher than that in PBMCs (Figure 1A). $CD8^+$ cells expressed a similar level of Munc13-4 protein as other PBMC cell types (Figure 1B). Similar amounts of platelet- and PBMC-derived proteins could be obtained from a sample (data not shown). Therefore, platelets were used to perform Western blotting to screen for Munc13-4 deficiency. Of the 85 patients screened, 6 patients were diagnosed with FHL3 (Figure 1C). Munc13-4 protein was barely detected in the platelets of each FHL3 patient regardless of the gene mutation (Table 1). For each sample, no more than 1 mL of whole blood was required to perform the analysis.

Difficulty in diagnosing FHL3 in the acute phase of the disease

Patients in the acute phase of the disease who require screening for FHL often receive platelet transfusions because of thrombocytopenia.[4-6] To study the effect of transfused platelets on screening results, FHL3 screening was attempted in a patient receiving platelet transfusions. As expected, Western blotting using platelets could not detect Munc13-4 deficiency because of the normal expression of the protein in the transfused platelets (Figure 2A left column). Surprisingly, Western blotting using PBMCs also could not clearly identify Munc13-4 deficiency because a substantial number of platelets were present in the PBMCs obtained by the standard method (Figure 2A right column). By positively selecting $CD45^+$ cells and removing platelets, it was found that a considerable amount of the Munc13-4 protein detected in PBMC samples

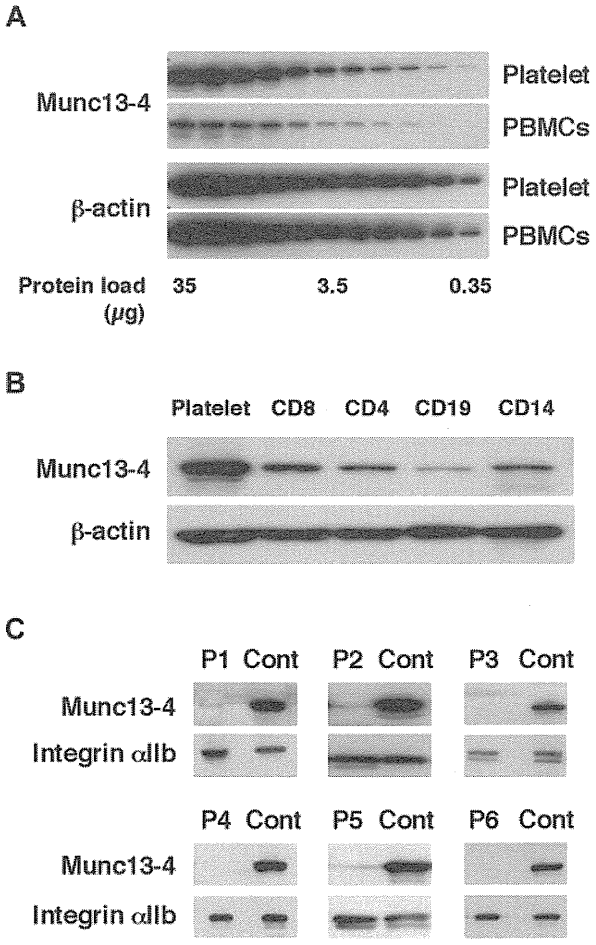

Figure 1. Diagnosing FHL3 by Western blotting using platelet protein. The amount of Munc13-4 protein expression was compared between platelets and PBMCs (A) and among platelets, $CD8^+$, $CD4^+$, $CD19^+$, and $CD14^+$ cells (B) by Western blotting. A representative result of 5 independent experiments is shown. (C) Six FHL3 patients were diagnosed by Western blotting for Munc13-4 protein using platelets.

obtained by standard density gradient centrifugation was actually derived from the contaminating platelets (Figure 2B).

We performed a NK-cell degranulation assay for every referred sample and found the assay to be defective for every FHL3 patient identified (data not shown). All of the other patients showed a normal release of lysosomal granules by NK cells; however, the analysis could not be performed in some patients because of the extremely low NK-cell number during the acute phase of the disease (data not shown).

We also examined the lysosomal granule release of platelets in 31 patients to determine whether this assay could be used as a screening method for FHL3. Lysosomal exocytosis of FHL3 platelets was partially impaired at steady state, but profound impairment was observed during the acute phase of the disease (Figure 3A-C). This profound impairment was also observed in platelets obtained from some secondary HLH patients during the acute phase (Figure 3B-C). These results indicate that it is difficult to diagnose FHL3 during the acute phase of HLH either by Western blot or by lysosomal degranulation assay.

Table 1. UNC13D gene mutations of FHL3 patients

Patient	Age at onset	Gender	Mutation	Genotype	Predicted effect
P1	14 days	Female	c.1596 + 1G → C	Homo	Splice error
P2	2 months	Male	c.322–1G → A	Hetero	Splice error
			c.990G → C	Hetero	p.Q330H
			c.3193C → T	Hetero	p.R1065X
P3	12 months	Female	c.754–1G → C	Hetero	Splice error
			c.2485delC	Hetero	p.L829fs
P4	4 months	Female	c.754–1G → C	Hetero	Splice error
			c.1799C → T	Hetero	p.T600M
			c.1803C → A	Hetero	p.Y601X
P5	2 months	Female	c.754–1G → C	Hetero	Splice error
			c.1596 + 1G → C	Hetero	Splice error
P6	5 months	Male	ND	ND	ND

Mutations were checked for single nucleotide polymorphisms using the dbSNP Build 132 database from the National Center for Biotechnology Information.

X indicates stop; fs, frame shift; and ND, not determined.

Rapid diagnosis of FHL3 by flow cytometric detection of intraplatelet Munc13-4

To overcome the difficulty in diagnosing FHL3 during the acute phase of HLH, antibodies were raised against the full-length human Munc13-4 protein (supplemental Figure 1) and a new method was developed to detect Munc13-4 protein in platelets by flow cytometry. A total of 35 patients, including 4 with FHL3 (P3-P6), were

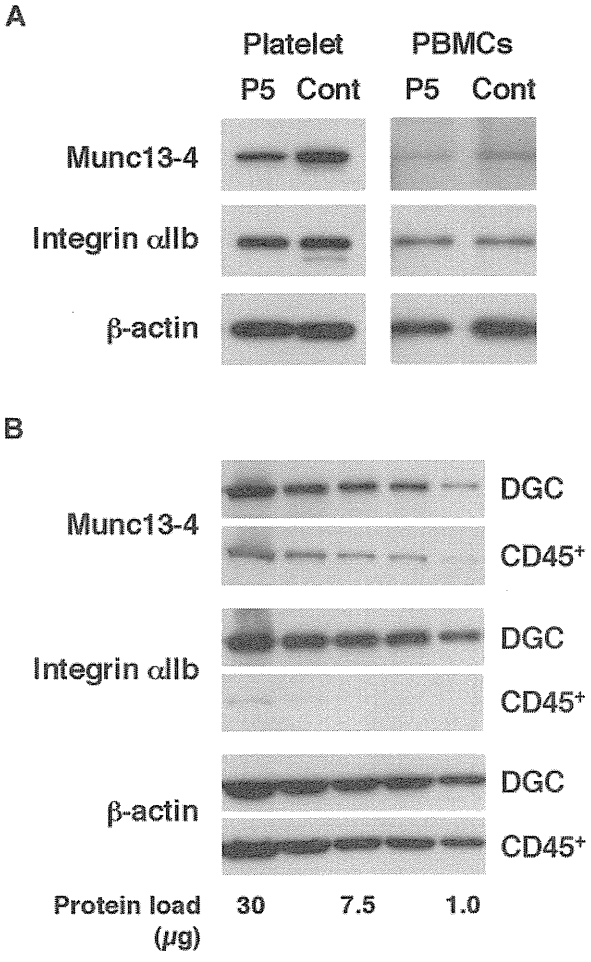

Figure 2. Effect of platelet transfusion on Western blot analysis. (A) Western blotting analysis for Munc13-4 expression using platelets and PBMCs from an FHL3 patient (P5) receiving platelet transfusions during the acute phase of the disease. (B) The expression of Munc13-4 was compared between PBMCs obtained by density gradient centrifugation (DGC) and $CD45^+$ cells obtained by magnetic sorting from healthy controls. A representative result of 3 independent experiments is shown.

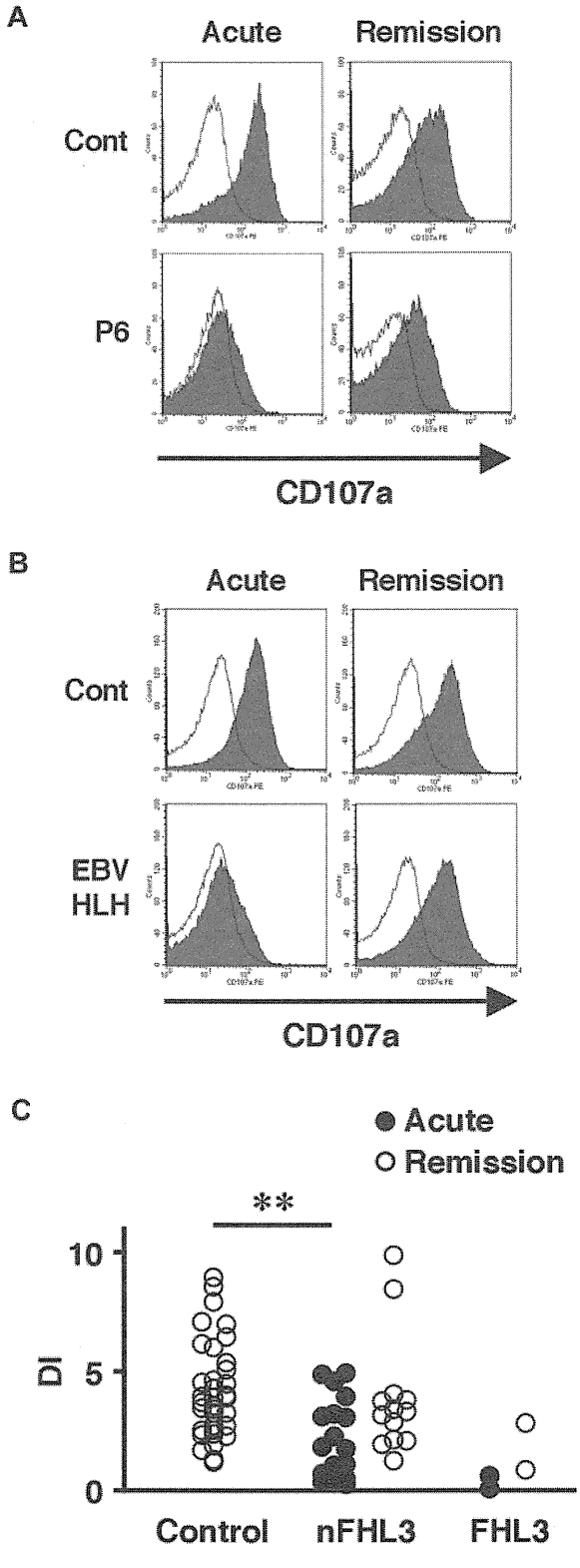

Figure 3. Analysis of lysosomal exocytosis using platelets from HLH patients. Platelets from an FHL3 patient (P6; A) and from a secondary (EBV-associated) HLH patient (B) along with healthy controls were left untreated (open histogram) or were stimulated with thrombin (closed histograms), and the surface expression of CD107a was analyzed by flow cytometry. Analysis was performed during the acute phase of the disease (left column) and after clinical remission (right column). (C) Degranulation index (DI) of platelets from HLH patients during the acute phase (●) and after clinical remission (○). HLH patients with normal NK-cell degranulation and Munc13-4 protein expression by Western blot analysis were defined as non-FHL3 (nFHL3). $^{**}P < .01$ by the Tukey post hoc test.

analyzed using this method. Munc13-4 deficiency was readily detected in all of the FHL3 patients, with a sample volume of < 100 μL of whole blood (Figure 4A-C). Munc13-4 protein was expressed at normal level in the platelets of parents and siblings of FHL3 patients carrying heterozygous *UNC13D* mutations (data not shown). In the FHL3 patient receiving platelet transfusions, flow cytometric analysis revealed bimodal populations of normal and Munc13-4–deficient platelets (P5 in Figure 4A). As shown in Figure 4B, the method was able to clearly identify Munc13-4–deficient platelets in whole blood samples stored at room temperature for 1 week.

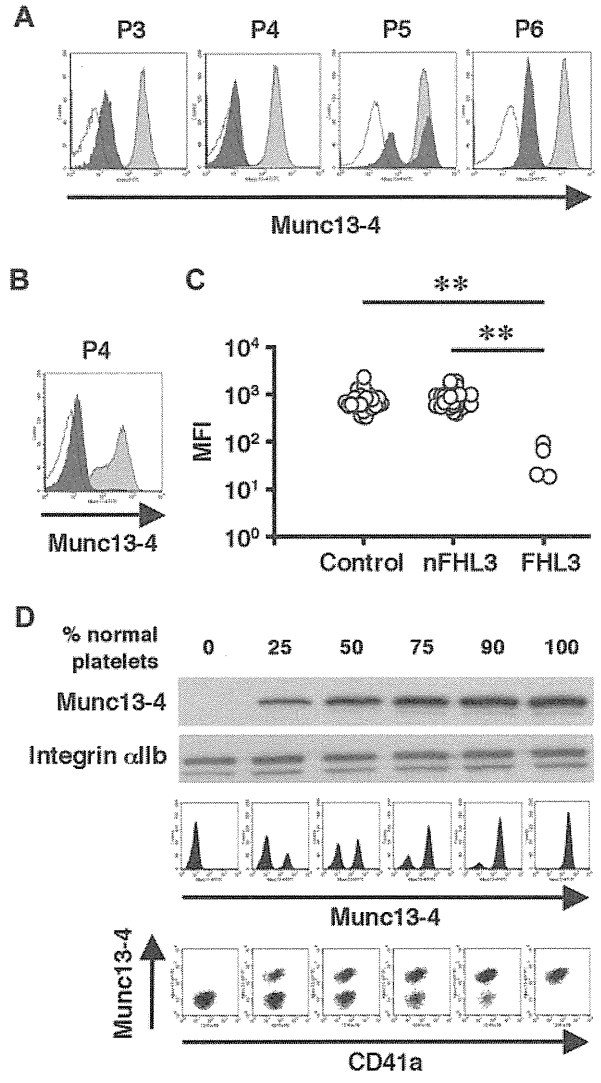

Figure 4. Flow cytometric detection of intraplatelet Munc13-4 protein. Flow cytometric analysis of intraplatelet Munc13-4 expression in 4 FHL3 patients and healthy controls using whole blood samples shipped overnight (A) and in an FHL3 patient (P4) and a healthy control using samples stored at room temperature for a week (B). Dark closed histograms represent platelets from FHL3 patients, whereas light closed histograms represent platelets from healthy controls. Open histograms represent staining with isotype controls. (C) Mean fluorescence intensity (MFI) of intraplatelet Munc13-4 staining for HLH patients and healthy controls. All of the healthy controls (n = 35) were adults. Non-FHL3 (nFHL3) patients (n = 31), as defined in Figure 3, varied in age (2 days-39 years) and included 2 patients with FHL2. Age-related variations in the MFI of Munc13-4 staining were not observed. $^{**}P < .01$ by the Tukey post hoc test. (D) The sensitivities of Western blot and flow cytometric analyses for detecting Munc13-4–deficient platelets were compared.

To determine the sensitivity of the new method, Munc13-4–deficient platelets were mixed with normal platelets at varying ratios. Western blot analysis could not detect Munc13-4–deficient platelets easily, even when the proportion of normal platelets was as low as 25% (Figure 4D). In contrast, flow cytometric analysis easily identified 10% Munc13-4–deficient platelets among 90% normal platelets (Figure 4D), which proved the high sensitivity of the method in diagnosing FHL3.

Discussion

FHL is a rare but life-threatening inherited immune disorder for which mutations in 4 genes have been identified as causative factors. *PRF1* encodes the cytolytic effector protein perforin that forms a pore-like structure in the target cell membrane.[1,12] A mutation in *PRF1* results in FHL2,[7] which accounts for 20%-50% of FHL cases.[4,5] *UNC13D* encodes the protein Munc13-4, which is crucial for the fusion of cytolytic granules to the plasma membrane and the subsequent release of perforin and granzymes.[1,12] Mutations in *UNC13D* result in FHL3,[8] which accounts for 20%-30% of FHL cases.[4,12] FHL4 is caused by mutations in *STX11*, which encodes syntaxin-11.[9] Mutations in *STXBP2*, which encodes Munc18-2, were recently reported to cause FHL5.[10,11] Syntaxin-11 and Munc18-2 also mediate the fusion of cytolytic granules to the plasma membrane.[1,5,12] The ability to screen for FHL2-5 rapidly would facilitate the initiation of life-saving immunosuppressive therapy and the preparation of FHL patients for hematopoietic stem cell transplantation.

In the present study, we found that the Munc13-4 protein is expressed abundantly in platelets (Figure 1A-B). The detection of Munc13-4 protein in platelets by Western blotting (Figure 1C) or flow cytometry (Figure 4A-B) was a reliable screening method to identify FHL3 patients. Munc13-4–deficient platelets were identified easily among normal transfused platelets by flow cytometry, which indicated that this method could be applied to patients who are receiving platelet transfusions during the acute phase of the disease (P5 in Figure 4A). Detection of intraplatelet Munc13-4 was enabled by the use of highly specific antibodies against the full-length human Munc13-4 (supplemental Figure 1).

There is a possibility that FHL3 patients with residual Munc13-4 protein expression could be overlooked by the screening methods described in this study. Most FHL3 patients have mutations that result in the absence or significant reduction of Munc13-4 protein expression,[16,23] as was the case with the patients screened in this study (Figure 1C), which suggests that the mutated Munc13-4 protein is unstable. The NK-cell degranulation assay, which was performed for every referred sample with a sufficient number of NK cells, revealed defective degranulation only in the identified FHL3 patients (date not shown). These results indicate that the majority of mutations in *UNC13D* are likely amenable to rapid detection by the new methods described in this study. Comparative studies on the *UNC13D* genotype, Munc13-4 protein expression, and the lysosomal exocytosis assay must be performed to confirm the reliability of these methods.

It was also investigated whether the analysis of lysosomal release by platelets could be used as an alternative method to screen for FHL3. Profound impairment of lysosomal exocytosis by platelets during the acute phase of the disease and restoration of this impairment after clinical remission was observed in FHL3 and in some secondary HLH patients (Figure 3). It is not clear whether this transient impairment of platelet degranulation is involved in HLH pathogenesis or if it merely reflects in vivo platelet activation by diffuse endothelial damage during the acute phase of the disease that renders them unresponsive to ex vivo stimulation. The release of lysosomal granules by Munc13-4–deficient platelets was impaired only minimally at steady state (Figure 3A and 3C), which is in contrast to a recent study showing the involvement of the Munc13-4 protein in the release of lysosomal granules in mouse platelets.[27] Although the precise reason for this discrepancy is unclear, platelet degranulation is likely to be regulated differentially between species; for example, Munc13-4–deficient mice have bruising and bleeding tendencies[27] that are not commonly associated with human FHL3. Further studies are warranted to elucidate the exocytosis pathways of platelets and their role in the pathophysiology of HLH.

With the development of tools for rapid screening, the diagnostic approach for FHL has changed over the years. Impaired NK cytotoxicity was the first reported signature clinical finding of FHL patients.[13,14] Defective CTL activity was subsequently reported as another hallmark of FHL.[7,8,16,28] However, NK-cell activity is also decreased in some cases of secondary HLH,[15,17-20] and the CTL cytotoxicity assay is not readily accessible to most clinicians. The NK-cell lysosomal exocytosis assay is a comprehensive method to identify patients with a degranulation defect.[10,11,22-24] However, this analysis is not available in some patients with extremely reduced NK-cell numbers, which are often observed during the acute phase of HLH.[19] Although CTLs can be an alternative tool to perform the lysosomal exocytosis assay,[24,28,29] it remains impossible to differentiate FHL3-FHL5.[10,11,23,24] Impairment in these assays warrants the genetic confirmation of FHL, but sequencing all of the candidate genes is not a suitable approach for rapid diagnosis. Flow cytometric detection of perforin expression in NK cells is a reliable and rapid way of identifying patients with FHL2,[21] and the new method described in this study for the detection of Munc13-4 expression in platelets would add to the rapid diagnosis of FHL3.

Platelets could also be used for the screening of FHL4 and FHL5 because they share some granule-transport mechanisms with other types of hematopoietic cells, including CTLs and NK cells.[2,30,31] Indeed, in the present study, both syntaxin-11 and Munc18-2 were expressed abundantly in platelets (data not shown). We are currently using platelet proteins to screen for FHL4-FHL5 by Western blot analysis, although no cases have been found so far because of the extreme rarity of these disorders.

In summary, platelets abundantly express Munc13-4 protein and are a useful tool to screen for FHL3. By detecting intraplatelet Munc13-4 expression by flow cytometry, it is now possible to rapidly screen for FHL3 with a very small sample of whole blood, even in the acute disease phase requiring platelet transfusion. Because platelets share some of their granule transport systems with other types of hematopoietic cells, they could also be used to screen for other types of immune disorders, including FHL4 and FHL5.

Acknowledgments

The authors are grateful to all of the participating patients, their families, and the referring physicians for their generous cooperation in this study.

This study was supported by grants from The Morinaga Foundation for Health and Nutrition; from the Japanese Ministry of